LETTERS

Mechanochemical analysis of DNA gyrase using rotor bead tracking

Jeff Gore[1]*, Zev Bryant[2,3]*†, Michael D. Stone[2]*†, Marcelo Nöllmann[2], Nicholas R. Cozzarelli[2] & Carlos Bustamante[1–4]

DNA gyrase is a molecular machine that uses the energy of ATP hydrolysis to introduce essential negative supercoils into DNA[1–3]. The directionality of supercoiling is ensured by chiral wrapping of the DNA[4,5] around a specialized domain[6–9] of the enzyme before strand passage. Here we observe the activity of gyrase in real time by tracking the rotation of a submicrometre bead attached to the side of a stretched DNA molecule[10]. In the presence of gyrase and ATP, we observe bursts of rotation corresponding to the processive, stepwise introduction of negative supercoils in strict multiples of two[11]. Changes in DNA tension have no detectable effect on supercoiling velocity, but the enzyme becomes markedly less processive as tension is increased over a range of only a few tenths of piconewtons. This behaviour is quantitatively explained by a simple mechanochemical model in which processivity depends on a kinetic competition between dissociation and rapid, tension-sensitive DNA wrapping. In a high-resolution variant of our assay, we directly detect rotational pauses corresponding to two kinetic substeps: an ATP-independent step at the end of the reaction cycle, and an ATP-binding step in the middle of the cycle, subsequent to DNA wrapping.

Negative DNA supercoiling is essential *in vivo* to compact the genome, to relieve torsional strain during replication, and to promote local melting for vital processes such as transcript initiation by RNA polymerase[12,13]. In bacteria, negative supercoiling is achieved through the activity of DNA gyrase, which works against mechanical stresses to drive the genome into an elastically strained configuration. Single-molecule techniques have yielded important insights into the mechanisms of other topoisomerases[14], but have yet to be applied to DNA gyrase.

Gyrase and other type II topoisomerases carry out a complex series of conformational changes resulting in the passage of an intact DNA duplex (the T-segment) through a transient break in another DNA duplex (the G-segment), changing the linking number[15] of the DNA by two[11]. Gyrase further embellishes this mechanism with a specialized adaptation whereby a chiral DNA wrap is formed before strand passage. The DNA wrap ensures the directionality of topoisomerization and confers on gyrase its unique ability to introduce, rather than merely to relax, DNA supercoils[4–9]. Wrapping involves a large change in the end-to-end extension of the DNA[7,16], and is therefore expected to be sensitive to tension and subject to perturbation in single-molecule assays. The equilibrium properties of DNA wrapped around gyrase or its subdomain have been studied extensively[4,5,7,8,16,17], but the dynamics of DNA wrapping remain largely uncharacterized. Other poorly understood aspects of gyrase dynamics include the mechanism of processivity (by which gyrase can perform many successive strand passages without releasing the DNA substrate), the location of the rate-limiting step for the overall reaction cycle, and the coupling between ATP consumption and supercoil introduction.

To dissect the mechanochemical cycle of DNA gyrase, we have used a method that we developed for measuring torque and changes in twist in a single DNA molecule in real time[10]. This rotor bead tracking technique requires a molecular construct containing three distinct chemical modifications (Fig. 1a). Tension is generated in the molecule by pulling at the two ends of the DNA, and the central 'rotor' bead is attached to the middle of the DNA just below an engineered single strand nick, which acts as a free swivel (Fig. 1b). The angle of the rotor bead then reflects changes in twist of the lower DNA segment, and the angular velocity of the bead is proportional to the torque in this segment. Previously we applied tension to the molecule using a laser trap[10], whereas here we use a magnetic tweezers[18,19] apparatus based on an inverted microscope (Fig. 1b). Tension in the DNA causes changes in linking number to partition into DNA twist[15,19], resulting in a torque on the rotor bead. An enzymatic process that changes the linking number by two will cause the rotor bead to spin around twice as the DNA returns to its equilibrium conformation. Thus, the DNA construct serves as a self-regenerating substrate for DNA gyrase.

In the absence of enzyme, the rotor bead fluctuates around a mean angle as a result of thermal noise[10]. On addition of *Escherichia coli* gyrase and 1 mM ATP, the rotor bead undergoes bursts of directional rotation (clockwise as viewed from below, as expected for negative supercoiling), separated by periods of inactivity (Fig. 1c). The pauses between bursts become longer as the enzyme concentration is reduced. We infer that a burst of rotation corresponds to the activity of a single enzyme that binds to the DNA, performs one or more catalytic cycles, and then dissociates. Each burst results in an even number of rotations (Fig. 1d), as predicted from the established sign-inversion mechanism of type II topoisomerases[11], in which a single catalytic cycle changes the DNA linking number by two.

As tension is varied from 0.35 to 1.3 pN, the activity of gyrase changes markedly (Figs 1c and 2a–c). Unexpectedly, the supercoiling velocity in a processive burst is not a strong function of template tension (Fig. 2a). However, processivity and initiation rate are sensitive to small changes in tension (Figs 1c and 2b, c). At 1 pN, gyrase activity consists almost exclusively of isolated single enzymatic cycles, whereas at lower force the bursts of rotation increase in length (Figs 1c and 2b). Burst initiation is also strongly suppressed by force: the waiting times between bursts increase by more than two orders of magnitude over a 0.5-pN range of tensions (Figs 1c and 2c).

[1]Department of Physics, University of California, Berkeley, California 94720, USA. [2]Department of Molecular and Cell Biology, University of California, Berkeley, California 94720, USA. [3]Physical Biosciences Division, Lawrence Berkeley National Laboratory, Berkeley, California 94720, USA. [4]Howard Hughes Medical Institute, USA. †Present addresses: Department of Biochemistry, Stanford University, Stanford, California 94305, USA (Z.B.); Department of Chemistry, Harvard University, Cambridge, Massachusetts 02138, USA (M.D.S.).
*These authors contributed equally to this work.

A simple mechanochemical model quantitatively explains these experimental results (Fig. 3). We consider a state ('gyrase–DNA') in which DNA is bound to the enzyme but not yet fully wrapped. We expect this state to be vulnerable to rapid dissociation because of its limited protein–DNA-binding interface and by analogy to yeast topoisomerase II, which dissociates from a 40-bp DNA segment at ~100 Hz (F. Mueller-Planitz and D. Herschlag, personal communication). According to our model, the gyrase–DNA complex undergoes a kinetic competition between DNA wrapping (which in the presence of ATP commits the enzyme to a productive cycle) and dissociation (which terminates a processive burst). At the end of each cycle, gyrase returns to the vulnerable state and must repeat its kinetic choice. In the absence of mechanical stresses, wrapping is very rapid, tending to outcompete dissociation and leading to processive supercoiling. Increased tensions slow down the DNA wrapping step, lengthening the time spent in the vulnerable state and increasing the probability of dissociation.

The average number of enzymatic cycles $\langle n \rangle$ in each burst of activity is given by $\langle n \rangle = 1/(1 - P_{\mathrm{cycle}})$, where

$$P_{\mathrm{cycle}}(F) = \frac{k_{\mathrm{wrap}}(F)}{k_{\mathrm{wrap}}(F) + k_{\mathrm{off}}}$$

is the probability of the gyrase–DNA complex committing to a productive catalytic cycle. Assuming a simple transition state model[20] with a distance to the transition state of Δx_t, the rate of wrapping is given by $k_{\mathrm{wrap}} = k_{\mathrm{wrap},0}\exp(-F\Delta x_t/k_{\mathrm{B}}T)$, where $k_{\mathrm{B}}T = 4.1$ pN nm is the thermal energy of the bath and F is the

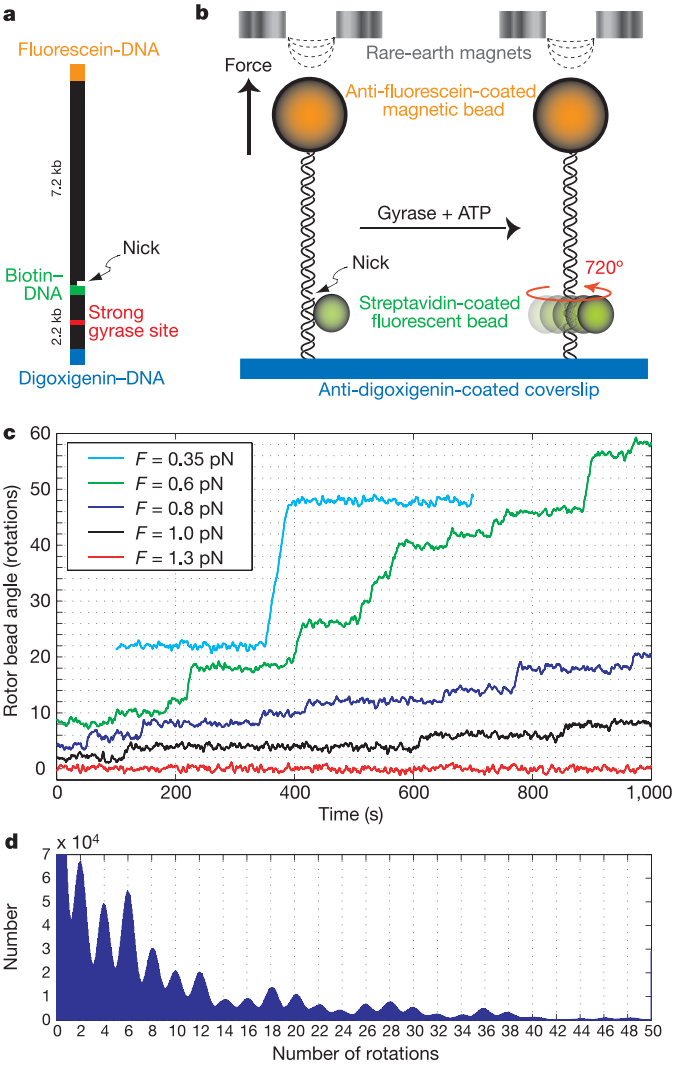

Figure 1 | Experimental design and single-molecule observations of gyrase activity. **a**, The molecular construct contains three distinct attachment sites and a site-specific nick, which acts as a swivel. A strong gyrase site was engineered into the lower DNA segment[29]. **b**, Molecule and bead assemblies were constructed in parallel in a flow chamber and assayed by using an inverted microscope equipped with permanent magnets. Each molecule was stretched between the glass coverslip and a 1-μm magnetic bead, and a 530-nm diameter fluorescent rotor bead was attached to the central biotinylated patch. In the presence of gyrase and ATP, the rotor bead underwent bursts of rotation due to the enzymatic activity of individual gyrase enzymes acting on the DNA segment below the rotor bead. **c**, Plot of the rotor bead angle as a function of time (averaged over a 2-s window), showing bursts of activity due to diffusional encounters of individual gyrase enzymes. The activity of the enzyme is strongly dependent on tension. With the exception of the one at 0.35 pN, the traces shown were taken in the same chamber with a single concentration of gyrase; thus, the differences in burst density reflect force-dependent initiation rates. **d**, Histogram of the pairwise difference distribution function summed over 11 traces of 15–20 min (averaged over a 4-s window) at forces of 0.6–0.8 pN. The spacing of the peaks indicates that each catalytic cycle of the enzyme corresponds to two full rotations of the rotor bead, as expected for a type II topoisomerase such as DNA gyrase.

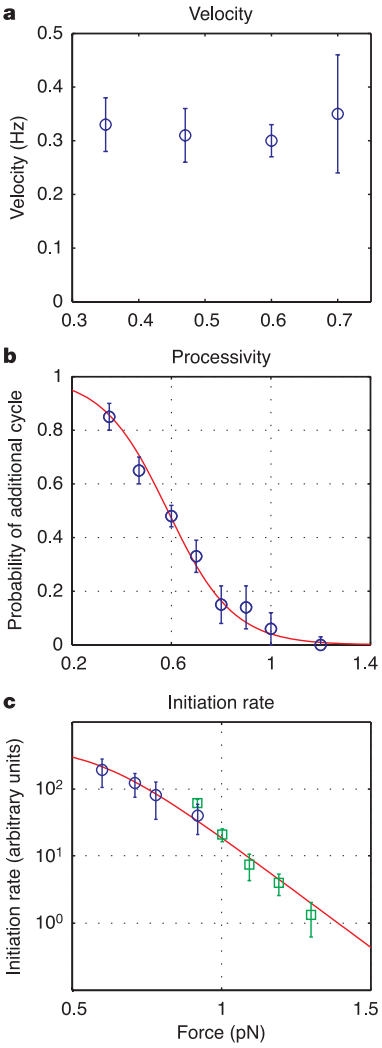

Figure 2 | Modulation of gyrase activity by DNA tension. The velocity (**a**) within a burst is insensitive to DNA tension, but both the processivity (**b**) and initiation rate (**c**) decrease rapidly as DNA tension increases. In **c**, tension-dependent initiation rates were measured in two independent experiments after the introduction of 10 nM (green squares) or 5 nM (blue circles) gyrase. Error bars indicate the s.e.m.

force applied to the magnetic bead. In our model, the observed burst frequency $k_{init} = [gyrase]k_{on}P_{cycle}$ decreases at higher force because of an increased number of 'invisible' gyrase–DNA binding events in which the enzyme dissociates before carrying out a single cycle. In Fig. 2b, c we fit $P_{cycle}(F)$ and $k_{init}(F)$ using the two parameters $\Delta x_t = 31 \pm 3$ nm and $k_{wrap,0}/k_{off} = 85 \pm 30$ (red line; see also Methods and Supplementary Note). This single pair of parameter values yields good fits to both processivity and initiation rate data, supporting the idea that a kinetic competition between wrapping and dissociation underlies both motor properties. The measured transition state distance of ~31 nm is close to the total expected decrease in DNA extension on wrapping of ~120 bp (~40 nm)[16].

Unlike DNA wrapping, the burst velocity is insensitive to tension (Figs 1c and 2a) and must be limited by the rate of some other, force-insensitive step. Having used mechanical perturbation[21] to characterize the wrapping step, we employed a complementary strategy to characterize the rate-determining step: direct observation of pauses in the reaction cycle[22,23]. We improved the time resolution of our assay by reducing the size of the rotor bead and shortening the torque-bearing DNA segment (see Methods). High-resolution traces (Fig. 4a) contain many distinct pauses within processive bursts. We tried to locate the position along the repeating 720° reaction coordinate at which the main pause in the cycle occurs. Most of the pronounced pauses occurred after two full rotations of the rotor bead (Fig. 4a and Supplementary Fig. 1). The remaining pauses occurred after about one rotation of the rotor bead (Fig. 4a, asterisks). A histogram of pause durations (Supplementary Fig. 1) confirms that the main pause (~1.5 s) is at the two-rotation mark, but suggests the possibility of a shorter (~0.8 s) pause in the middle of the cycle.

The positions of intraburst pauses indicate that the principal rate-determining step occurs near the beginning or the end of the reaction cycle. DNA wrapping lies at the beginning of the cycle, but we have already shown that this step is not rate-limiting. We therefore conclude that the rate-limiting step occurs at the end of the cycle (denoted k_{rl} in Fig. 3). The shorter, mid-cycle pause might correspond to an intermediate following DNA wrapping and preceding strand passage. Exit from this intermediate is expected to depend on ATP, because ATP binding is required for strand passage[24,25] but not for DNA wrapping[5] (Fig. 3). To directly investigate the role of ATP in the cycle, we carried out high-resolution assays at varying ATP concentrations. In the complete absence of ATP, the cycle should

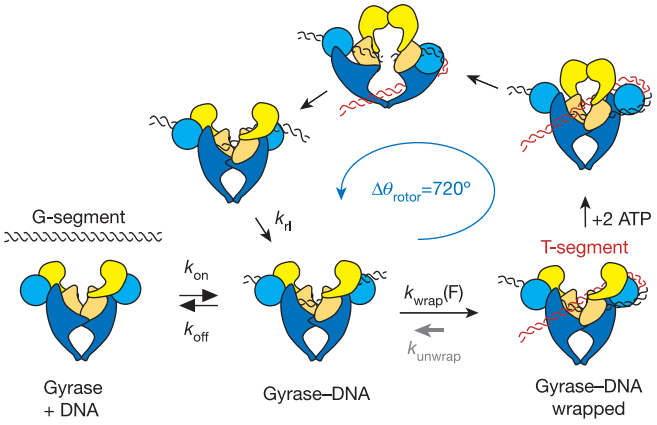

Figure 3 | Proposed mechanochemical model. From the state labelled 'gyrase–DNA', there is a kinetic competition between DNA wrapping and dissociation. Wrapping is strongly inhibited by DNA tension. After wrapping and ATP binding, the enzyme is committed to a full catalytic cycle in which two negative supercoils are introduced to the DNA, causing the rotor bead to spin by $\Delta\theta = 720°$. At saturating concentrations of ATP, unwrapping (small arrow labelled k_{unwrap}) is negligible; however, see Fig. 4b, c.

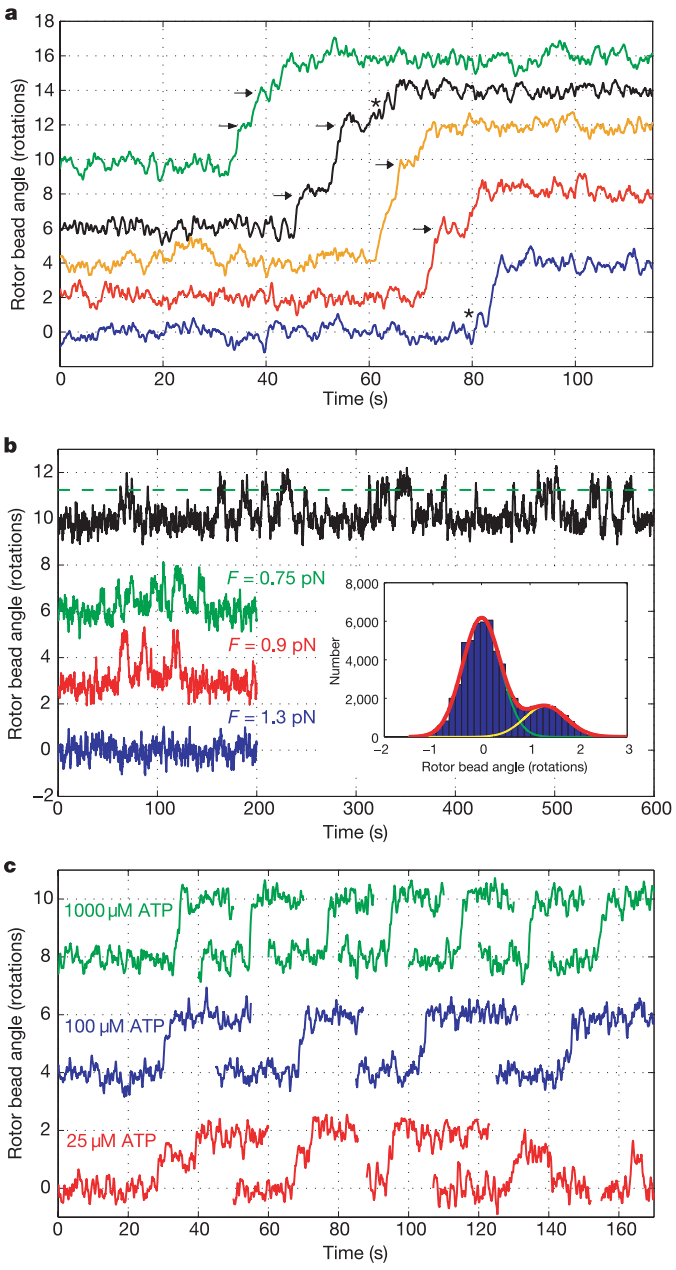

Figure 4 | Gyrase activity observed at high resolution. **a**, High-resolution traces ($F \approx 0.8$ pN) at 1 mM ATP show that the dominant pause in the catalytic cycle occurs at the two-rotation mark, corresponding to either the beginning or the end of the cycle (arrows). Pauses were less frequently observed in the middle of the catalytic cycle (asterisks). Traces were averaged over a 300-ms window. Burst velocity in the high-resolution assay was 0.38 ± 0.04 Hz (mean ± s.e.m.), which was not significantly faster than in the low-resolution assay (0.32 ± 0.03 Hz, Fig. 2a). **b**, In the absence of ATP, the rotor bead angle alternates between two values, as expected for reversible DNA wrapping (black trace, $F = 0.9$ pN). The wrapped state corresponds to a change in the angle of the rotor bead of ~1.3 rotations (broken green line), as shown by a double-gaussian fit to the histogram of rotor bead angles for this trace (inset). Increasing the DNA tension from 0.75 pN (green trace) to 1.3 pN (blue trace) strongly inhibits wrapping. **c**, Fine structure of isolated enzymatic cycles at several ATP concentrations. The mid-cycle pause at about the one-rotation mark becomes more pronounced as the ATP concentration is lowered, revealing an ATP-binding step subsequent to DNA wrapping (green traces, 1 mM ATP; blue traces, 100 μM ATP; red traces, 25 μM ATP). At 25 μM ATP, unwrapping often occurs before the cycle can be completed (final red traces).

halt at the wrapped intermediate ('gyrase–DNA wrapped' in Fig. 3), after roughly one rotation of the rotor bead[5]. The wrapped state should persist until a rare unwrapping event occurs (k_{unwrap} in Fig. 3), returning the rotor bead to its original position.

As predicted from this model, we observed reversible rotations of the rotor bead when low concentrations of gyrase were introduced in the absence of ATP (Fig. 4b). The change in angle of the rotor bead on wrapping is ~1.3 rotations (Fig. 4b, inset), slightly larger than the value (0.8 rotations) predicted from bulk topoisomerase I protection assays[17]. This discrepancy may be due to the difficulty of estimating the number of bound enzymes in bulk experiments. The wrapped state is long-lived (with a mean lifetime of 7 s at $F = 0.9$ pN, $N = 66$), in accordance with a primary assumption of our mechanochemical model: namely, the wrapped and unwrapped states are not in rapid equilibrium. As expected from our model, wrapping events are strongly suppressed by tension (Fig. 4b).

At subsaturating ATP concentrations, the cycle can progress to completion only on ATP binding. Lowering the ATP concentration should therefore lengthen the time spent in a wrapped intermediate state. This prediction is confirmed by observations of single enzymatic cycles at varying ATP concentrations in the high-resolution assay (Fig. 4c). At saturating ATP, a pause at the one-rotation mark is only rarely observed. As the ATP concentration is reduced, the mid-cycle pause becomes clearly visible. At 25 μM ATP, unwrapping often occurs before the catalytic cycle can be completed, reflecting a kinetic competition between unwrapping and ATP binding (Fig. 4c, final red traces).

Chiral DNA wrapping enables gyrase to introduce essential negative supercoils into the bacterial genome[18]. We have found that this wrapping step is rapid and exquisitely sensitive to tension in the DNA. Forces of ~1 pN (small in comparison to the >20 pN stall forces of DNA-based motors such as RNAP[20] and FtsK[26]) are sufficient to inhibit DNA wrapping by a factor of ~1,000. Rapid wrapping is essential for processivity, illustrating a general design principle for processive motors[27,28]: any on-pathway state that is vulnerable to dissociation requires a mechanism for rapid exit from this state into a more tightly bound configuration.

Because DNA wrapping is chiral, it is expected to be sensitive to torque as well as tension. Evidence for torque sensitivity can be seen in the difference in processivity between the high- and low-resolution assays: high-resolution traces taken over a range of forces (0.65–0.9 pN) show enhanced processivity (with the tension at the midpoint $P_{\mathrm{cycle}}(F) = 0.5$ shifted upwards by ~0.15 pN), suggesting that wrapping is decelerated by the small amount of torque (~3 pN nm) that accumulates owing to rotational drag in the low-resolution assay.

Direct detection of pauses in the supercoiling reaction by the high-resolution rotor bead tracking experiments presented here has shown that the rate-limiting step lies at the end of the cycle. Identifying the chemical and conformational nature of this 'reset' step presents a future challenge for biophysical investigations of DNA gyrase. A second, mid-cycle pause is directly observed at low ATP concentrations and corresponds to an intermediate awaiting ATP binding subsequent to DNA wrapping. Further studies of the drug and nucleotide dependence of the primary and secondary pauses[22] will illuminate the important issue of coupling between ATP turnover and DNA supercoiling.

METHODS

Molecular constructs and beads. Modified DNA constructs for rotor bead tracking were prepared as described[10], with the torsionally constrained DNA segment replaced by a 2.2 kb (low-resolution) or 1.1 kb (high-resolution) fragment derived from pMP1000 (a gift from P. Higgins), a plasmid containing the nuB 74 variant of the strong gyrase site from μ phage DNA[29]. We coated 1-μm magnetic beads (Dynal) with rabbit anti-fluorescein (Molecular Probes). We used streptavidin-coated 'Dragon Green' 0.53-μm rotor beads (Bangs Labs) or avidin-coated 'Yellow' nominal 0.46-μm rotor beads (Spherotech) fluorescent particles.

Chamber preparation. Flow chambers were prepared as described[10] and incubated for ~4 h with 0.2 mg ml^{-1} of anti-digoxigenin (Roche) in PBS followed by >8 h with a passivation buffer made by mixing equal volumes of 10 mg ml^{-1} of bovine serum albumin (BSA; NEB) and 80 mM Tris-HCl (pH 8.0), 1 M NaCl, 0.04% azide and 0.4% Tween-20. Molecule–bead assemblies were generated by successively incubating the chamber with DNA (~4 pM, 30 min), fluorescent beads (2 h) and magnetic beads (1 h) in binding buffer (40 mM Tris-HCl, 500 mM NaCl, 0.02% azide, 0.2% Tween-20 and 500 μg ml^{-1} of BSA; pH 8.0).

Microscopy. Single-molecule experiments were conducted on a modified Axiovert 100A inverted microscope (Zeiss) with a pair of neodymium–iron–boron magnets (Radio Shack) suspended above the flow chamber. The force on the magnetic bead was varied by raising or lowering the magnets. Brightfield images of magnetic beads or fluorescence images of rotor beads were imaged on an IXON electron-multiplying CCD camera (Andor). Forces (±20%) were determined by measuring the transverse fluctuations of the magnetic bead[19]. Movies of rotor beads were recorded at 40 Hz (100 Hz for the high-resolution experiments) for subsequent video analysis. The centroid of the fluorescent bead was determined with an accuracy of ~10 nm per frame, which translates into an error in the angle of ~3° (0.05 rad). In the low-resolution assay, the variance in the bead angle was 8 rad^2 with a relaxation time of 1.5 s. In the high-resolution assay, the variance was reduced to 4.5 rad^2 with a relaxation time of ~400 ms. Distinguishing between two angles of the rotor bead that are one rotation apart therefore requires ~1 s.

Experimental protocol. After flushing the channel with binding buffer, magnets were placed above the chamber and ~5 nM gyrase was added to the chamber in reaction buffer (35 mM Tris-HCl, 24 mM potassium glutamate, 4 mM $MgCl_2$, 2 mM dithiothreitol, 100 μg ml^{-1} of BSA and 0.2 mM spermidine; pH 7.6) containing 1 mM ATP. All saturating ATP data were taken with enzyme provided by A. Maxwell and all other data were taken with enzyme provided by J. Berger. All experiments were done at room temperature (23 ± 2 °C). The ATP concentration in the low ATP experiments was kept constant by adding an ATP regeneration system containing 10 mM phosphocreatine and 1.23 μM creatine phosphokinase. Activity in the chamber (burst density) for a given concentration of gyrase was variable and fell off over the course of hours, probably owing to inactivation and sticking of the enzyme to the chamber walls. To control for effective gyrase concentration, comparisons of burst (Fig. 2c) and wrapping (Fig. 4b) initiation rates were done in a single chamber by alternating forces without reintroducing enzyme.

Data analysis. Burst velocities were measured by a piecewise linear fit to the raw angle data for each burst containing four or more catalytic cycles. Mean velocities were calculated by summing the total number of cycles in all the bursts (typically $N \approx 50$ at each force) and dividing by the total time of all the bursts. Processive bursts in the low-resolution assay could be analysed only for forces between 0.3 pN and 0.7 pN. Forces below 0.3 pN are inaccessible because lateral fluctuations of the DNA interfere with tracking of the rotor bead. At forces above 0.7 pN, processive bursts become too rare to measure a velocity.

The average burst length $\langle n \rangle$ was calculated by adding the total number of enzymatic cycles completed at a given force and dividing by the total number of bursts at that force. Processivity was then plotted as $P_{\mathrm{cycle}} = 1 - 1/\langle n \rangle$. Initiation rate as a function of force was measured in two separate experiments (using 5 nM or 10 nM gyrase) for the low-force and high-force regimes. Initiation rates for each data set were multiplied by a fit scaling factor (related to the effective concentration) before plotting.

Received 13 June; accepted 11 October 2005.

1. Gellert, M., Mizuuchi, K., O'Dea, M. H. & Nash, H. A. DNA gyrase: an enzyme that introduces superhelical turns into DNA. *Proc. Natl Acad. Sci. USA* **73,** 3872–3876 (1976).
2. Champoux, J. J. DNA topoisomerases: structure, function, and mechanism. *Annu. Rev. Biochem.* **70,** 369–413 (2001).
3. Corbett, K. D. & Berger, J. M. Structure, molecular mechanisms, and evolutionary relationships in DNA topoisomerases. *Annu. Rev. Biophys. Biomol. Struct.* **33,** 95–118 (2004).
4. Liu, L. F. & Wang, J. C. DNA–DNA gyrase complex: the wrapping of the DNA duplex outside the enzyme. *Cell* **15,** 979–984 (1978).
5. Liu, L. F. & Wang, J. C. *Micrococcus luteus* DNA gyrase: active components and a model for its supercoiling of DNA. *Proc. Natl Acad. Sci. USA* **75,** 2098–2102 (1978).
6. Reece, R. J. & Maxwell, A. The C-terminal domain of the *Escherichia coli* DNA gyrase A subunit is a DNA-binding protein. *Nucleic Acids Res.* **19,** 1399–1405 (1991).
7. Corbett, K. D., Shultzaberger, R. K. & Berger, J. M. The C-terminal domain of DNA gyrase A adopts a DNA-bending β-pinwheel fold. *Proc. Natl Acad. Sci. USA* **101,** 7293–7298 (2004).

8. Ruthenburg, A. J., Graybosch, D. M., Huetsch, J. C. & Verdine, G. L. A superhelical spiral in the *Escherichia coli* DNA gyrase A C-terminal domain imparts unidirectional supercoiling bias. *J. Biol. Chem.* **280,** 26177–26184 (2005).
9. Kampranis, S. C. & Maxwell, A. Conversion of DNA gyrase into a conventional type II topoisomerase. *Proc. Natl Acad. Sci. USA* **93,** 14416–14421 (1996).
10. Bryant, Z. *et al.* Structural transitions and elasticity from torque measurements on DNA. *Nature* **424,** 338–341 (2003).
11. Brown, P. O. & Cozzarelli, N. R. A sign inversion mechanism for enzymatic supercoiling of DNA. *Science* **206,** 1081–1083 (1979).
12. Levine, C., Hiasa, H. & Marians, K. J. DNA gyrase and topoisomerase IV: biochemical activities, physiological roles during chromosome replication, and drug sensitivities. *Biochim. Biophys. Acta* **1400,** 29–43 (1998).
13. Wang, J. C. Cellular roles of DNA topoisomerases: a molecular perspective. *Nature Rev. Mol. Cell. Biol.* **3,** 430–440 (2002).
14. Charvin, G., Strick, T. R., Bensimon, D. & Croquette, V. Tracking topoisomerase activity at the single-molecule level. *Annu. Rev. Biophys. Biomol. Struct.* **34,** 201–219 (2005).
15. Bates, A. D. & Maxwell, A. *DNA Topology* (Oxford Univ. Press, Oxford, 2005).
16. Heddle, J. G., Mitelheiser, S., Maxwell, A. & Thomson, N. H. Nucleotide binding to DNA gyrase causes loss of DNA wrap. *J. Mol. Biol.* **337,** 597–610 (2004).
17. Kampranis, S. C., Bates, A. D. & Maxwell, A. A model for the mechanism of strand passage by DNA gyrase. *Proc. Natl Acad. Sci. USA* **96,** 8414–8419 (1999).
18. Smith, S. B., Finzi, L. & Bustamante, C. Direct mechanical measurements of the elasticity of single DNA molecules by using magnetic beads. *Science* **258,** 1122–1126 (1992).
19. Strick, T. R., Allemand, J. F., Bensimon, D., Bensimon, A. & Croquette, V. The elasticity of a single supercoiled DNA molecule. *Science* **271,** 1835–1837 (1996).
20. Wang, M. D. *et al.* Force and velocity measured for single molecules of RNA polymerase. *Science* **282,** 902–907 (1998).
21. Keller, D. & Bustamante, C. The mechanochemistry of molecular motors. *Biophys. J.* **78,** 541–556 (2000).
22. Yasuda, R., Noji, H., Yoshida, M., Kinosita, K. Jr & Itoh, H. Resolution of distinct rotational substeps by submillisecond kinetic analysis of F_1-ATPase. *Nature* **410,** 898–904 (2001).
23. Uemura, S., Higuchi, H., Olivares, A. O., De La Cruz, E. M. & Ishiwata, S. Mechanochemical coupling of two substeps in a single myosin V motor. *Nature Struct. Mol. Biol.* **11,** 877–883 (2004).
24. Roca, J. & Wang, J. C. The capture of a DNA double helix by an ATP-dependent protein clamp: a key step in DNA transport by type II DNA topoisomerases. *Cell* **71,** 833–840 (1992).
25. Baird, C. L., Harkins, T. T., Morris, S. K. & Lindsley, J. E. Topoisomerase II drives DNA transport by hydrolyzing one ATP. *Proc. Natl Acad. Sci. USA* **96,** 13685–13690 (1999).
26. Pease, P. J. *et al.* Sequence-directed DNA translocation by purified FtsK. *Science* **307,** 586–590 (2005).
27. Block, S. M. Leading the procession: new insights into kinesin motors. *J. Cell Biol.* **140,** 1281–1284 (1998).
28. Vale, R. D. Myosin V motor proteins: marching stepwise towards a mechanism. *J. Cell Biol.* **163,** 445–450 (2003).
29. Pato, M. L., Howe, M. M. & Higgins, N. P. A DNA gyrase-binding site at the center of the bacteriophage μ genome is required for efficient replicative transposition. *Proc. Natl Acad. Sci. USA* **87,** 8716–8720 (1990).

Supplementary Information is linked to the online version of the paper at www.nature.com/nature.

Acknowledgements We thank N. Crisona, P. Arimondo, A. Vologodskii, A. Edelstein, S. Mitelheiser, A. Schoeffler, and F. Mueller-Planitz for discussions; A. Maxwell and J. Berger for enzymes; P. Higgins for plasmids; and C. Hodges, M. Le and D. Jennings for technical assistance. J.G. acknowledges funding from the Hertz Foundation. This work was supported by the NIH and the DOE.

Author Information Reprints and permissions information is available at npg.nature.com/reprintsandpermissions. The authors declare no competing financial interests. Correspondence and requests for materials should be addressed to C.B. (carlos@alice.berkeley.edu) or N.R.C. (ncozzare@berkeley.edu).